Novel Green TiO_2 Nanoparticles from Corchorus olitorius leaf extract for Solar and UV Photocatalytic Degradation of Methylene blue and Tetracycline

Asmaa Deiaa Nusseif

asmaadeiaa@uomustansiriyah.edu.iq

Mustansiriyah University

Raad S. Sabry

Mustansiriyah University

Nedal A. Hussain

Mustansiriyah University

Ali N. Majeed

Scientific Research Commission

Research Article

Keywords: Green synthesis, TiO2 NPs, Corchorus olitorius, Photocatalytic, Methylene blue, Tetracycline

Posted Date: April 6th, 2026

DOI: https://doi.org/10.21203/rs.3.rs-9214743/v1

Additional Declarations: No competing interests reported.

Novel Green TiO_2 Nanoparticles from *Corchorus olitorius* leaf extract for Solar and UV Photocatalytic Degradation of Methylene blue and Tetracycline

Asmaa Deiaa Nusseif [a*], Raad S. Sabry [a], Nedal A. Hussain[a] and Ali N. Majeed[b]

[a] Department of Physics, College of Science, Mustansiriyah University, Falastin St, Baghdad,10052, Iraq.

[b] Scientific Research Commission, Baghdad, Iraq.

*Corresponding author: Asmaa Deiaa Nusseif

E-mail addresses: asmaadeiaa@uomustansiriyah.edu.iq.

Orcid ID: 0000-0001-5278-9910

corresponding author's phone number: +9647901964756

Co- author E-mail addresses and Orcid ID

1- Raad S. Sabry : drraad_sci@uomustansiriyah.edu.iq

Orcid ID: 0000-0001-6811-7799

2- Nedal A. Hussain: nedalali44@uomustansiriyah.edu.iq

Orcid ID: 0000-0001-7631-0230

3- Ali N. Majeed: ali.n.majeed@src.edu.iq

Acknowledgments:

The authors offer their sincere gratitude to the Department of Physics, College of Science, Mustansiriyah University, Bagdad, Iraq for their support.

Novel Green TiO_2 Nanoparticles from *Corchorus olitorius* leaf extract for Solar and UV Photocatalytic Degradation of Methylene blue and Tetracycline

Abstract:

Titanium dioxide nanoparticles (TiO_2 NPs) were synthesized via environmentally friendly approach using *Corchorus olitorius* (also known as Molokhia) leaf extract. This represents the first enquiry into *Corchorus olitorius* plant for the green synthesis of TiO_2. Several tests were used to characterize the prepared nanoparticles. XRD revealed the formation of anatase phase with a tetragonal structure and average crystallite sizes of 7.45 nm and 9.03 nm, calculated using Scherer equation and Williamson-Hall method, respectively. FTIR analysis confirming the presence of phytochemicals in *Corchorus olitorius* leaf extract as well as the formation of TiO_2 NPs. FESEM analysis revealed a microporous structure consisting of a regular distribution of spherical nanoparticles with an average particle size of 20 nm. Purity of TiO_2 NPs was confirmed by the presence of only titanium and oxygen elements, through EDX analysis. Defect related states was investigated by PL test. UV-Vis spectroscopy showed a broad absorption peak in the UV region with energy gap of 3.26 eV. TiO_2 NPs exhibited a high negative zeta potential of -31.8 mV, confirming their high stability in colloidal solution. The photocatalytic activity of TiO_2 NPs was investigated against Methylene blue (MB)dye and Tetracycline (TC) antibiotic. Greenly synthesized TiO_2 NPs exhibited highly photocatalytic activity with degradation efficiency of 97.5 %for MB and 56% for TC under sunlight which was not reported yet to the best of our knowledge. These results open up new horizons in the field of preparing nanomaterials and employing them to solve environmental problems in inexpensive and environmentally friendly ways.

Keywords: Green synthesis; TiO_2 NPs; *Corchorus olitorius*; Photocatalytic; Methylene blue; Tetracycline

Graphical abstract:

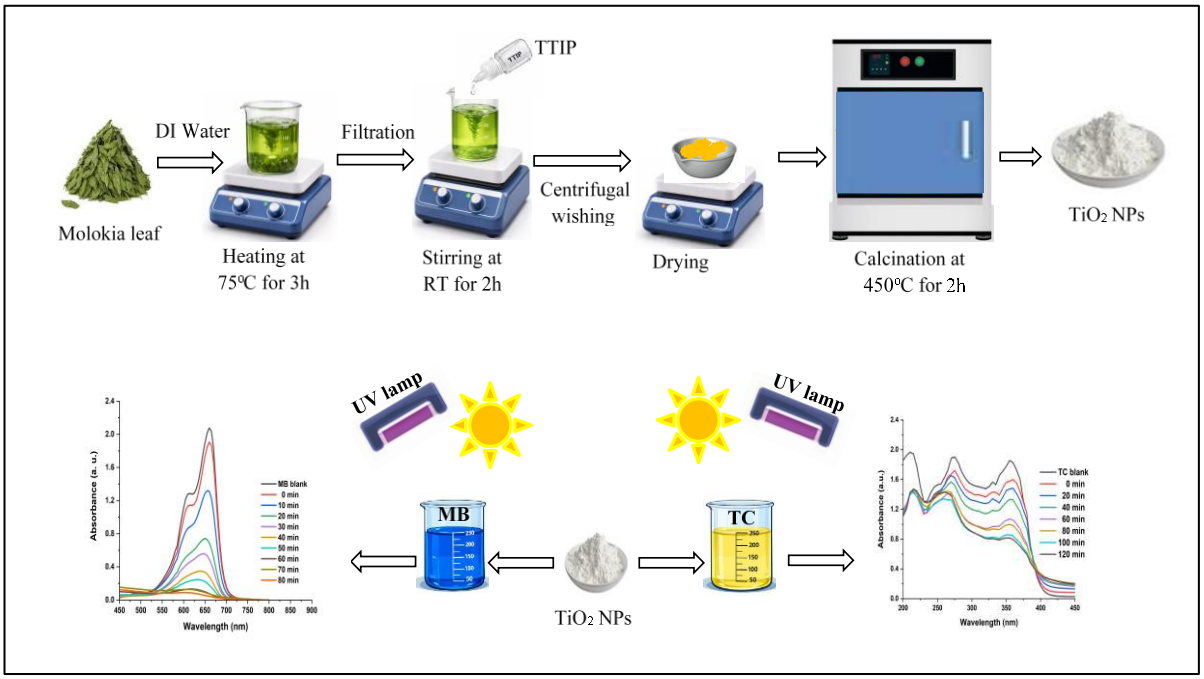

1- Introduction:

In the current era, the world is facing an unprecedented increase in water pollution as a result of population expansion and industrial development. Untreated pollutants, including organic dyes, antibiotics, and chemicals, find their way into water sources, posing a significant threat to human health and other living organisms [1-3]. Commercial dyes are regarded as one of the most hazardous pollutants owing to their significant chemical stability and highly resistant to degradation [4]. Methylene blue (MB), a cationic synthetic dye, is the most widely used dye in many industries for coloring, such as textile, plastic, and paper, which has led to its abundance in many industrial wastes [5]. The highly toxic and chemically stable of MB dye makes its removal from wastewater a challenging task. On the other hand, water contamination with antibiotics is an important issue that must be considered [6]. Tetracycline (TC) is the second most widely used antibiotic in the world for treating diseases in both humans and animals due to its broad antimicrobial spectrum and low cost [7]. Approximately 50-80% of tetracycline is released into the environment in its active form because it is difficult to metabolize and therefore is not digested in the bodies of humans or animals [8]. The continued discharge of antibiotics into the environment through wastewater from hospitals, poultry farms, and livestock is a major cause of antibiotic resistance, which poses a serious health threat to both ecosystems and humans [9,10].

In light of the above, researchers and scientists have intensified their efforts to find effective solutions to address water pollution. Several physical, chemical, and biological techniques are employed to treat contaminated water, including conventional adsorption, membrane filtration, irradiation, and microbiological or enzymatic decomposition [11-14]. However, these procedures are insufficiently effective in eliminating pollutants, underlining the need for more advanced and effective treatment strategies. Photocatalysis has emerged as promising approach for water remediation compared to other traditional methods [15,16]. Photocatalysis relies on the activation of semiconductor materials through absorb photons with energy equal or greater than to their bandgap to generate charge carriers which mediate redox reactions, that decomposes pollutants into harmless byproducts, such as carbon dioxide and water [17,18]. This approach offers environmentally friendly and cost-effective solution, especially when harness renewable solar energy [19].

In the past decade, many semiconductor nanomaterials, and particularly metal oxides, have been used as photocatalysts, and their photocatalytic activity has been exploited for the removal of pollutants such as TiO_2, ZnO, SnO_2, and CdS, among others [20-23]. TiO_2 has received significant attention due to its unique properties and wide range of applications, especially in the environmental domain [24-26]. TiO_2 is an n-type semiconductor with a wide band gap of 3.0-3.2 eV in its bulk counterpart, depending on its polymorphic. It exists in three polymorphic crystal structures known as anatase, rutile, and brookite [27]. TiO_2 as a photocatalyst has shown great potential for the removal of organic contaminants due to its high photocatalytic activity, chemical stability, non-toxic properties, and low cost [28,29]. Therefore, TiO_2 represents a particularly important option and remains more economically advantageous than other metal oxides for wastewater treatment.

Pure titanium dioxide exhibits low degradation efficiency towards organic pollutants due to its wide band gap and fast recombination of photo-generated electron –hole pairs [30,31]. Little reports are found in the literature that investigated the catalytic activities of pure TiO_2 nanoparticles using direct sunlight. Pure titanium dioxide achieves a degradation efficiency of 68.2% for MB dye under simulated sunlight after 60 min of illumination [32]. A 75.1% decomposition of the methylene blue solution (10 mg/L) was achieved using pure TiO_2 under sunlight after 90 minutes [33]. Pure titanium dioxide showed a weak degradation efficiency of 40.72% for tetracycline (50 mg/L) when exposed to ultraviolet radiation for 120 minutes [34], while no degradation was observed for tetracycline (10 mg/L) after 60 minutes of exposure to sunlight [35].

The decomposition efficiency of pure TiO_2 can increase depending on several factors, including crystal phase, crystallinity, particle size, surface area, surface morphology, and hydroxyl groups present on its surface. The anatase phase is known to be the most active phase of titanium dioxide compared to other phases; therefore, obtaining titanium dioxide in this phase can enhance its photocatalytic activity [36]. Microwave-assisted green synthesized TiO_2 NPs resulting in anatase phase exhibiting 97% decomposition activity of methylene blue after 90 minutes under sun light [37]. Another factor that plays

a crucial role in photocatalysis is particle size. The smaller the particle size, the greater the surface area, which increases the number of active sites available for photocatalytic reactions [38,39]. Eco-friendly synthesized TiO_2 NPs using *Beta vulgaris* extract with an average particle size of about 12 nm showed high efficacy, achieving a 91.41% degradation efficiency of methylene blue dye within 195 minutes of exposure to sunlight [40]. A vital role in enhancing the efficiency of pure titanium oxide can be attributed to the surface morphology. Some nanostructures have a higher capacity than others to transport electrons photoinjected into the crystal lattice of titanium dioxide [41]. Meanwhile, the generation of surface defects on the TiO_2 surface, such as oxygen vacancies and Ti^{3+}, inhibiting the recombination of photo-generated electron–hole pairs, which plays an important role in improving photocatalysis [42,43]. Also, the presence of functional groups on the surface of catalysts promotes the production of reactive oxygen species (OH and O_2^-), which helps in the breakdown of pollutants [44]. finally, the colloidal stability and dispersion of nanoparticles offering more exposed and accessible active sites, further increasing their photocatalytic performance [45]. Green-synthesized TiO_2 nanoparticles exhibit superior photocatalytic efficacy in the degradation of diverse organic dyes and pharmaceutical contaminants in wastewater, frequently outperforming conventionally synthesized TiO_2 where greenest synthesis methods produce the anatase phase with small particle sizes due to phytochemical capping agents, resulting in a large surface area in addition to the presence of functional groups on their surface. [46-48].

Green synthesis methods have gained significant popularity as a sustainable alternative to conventional chemical and physical synthesis methods [49]. Green synthesis refers to a sustainable and environmentally friendly method of synthesizing nanoparticles using natural sources, reducing the risks of chemicals used in traditional methods, as well as the resulting toxic waste. Green synthesis relies on natural extracts from various sources like plants, bacteria, fungi, and algae [50]. The widespread availability and low cost of these raw materials make their use sustainable and economical. Plants are more convenient because they are easy to obtain and use directly without any complicated procedures, as different parts of the plant can be used such as leaves, fruits, roots, bark, etc. [51]. Plant extracts are rich in phytochemicals such as phenolic compounds, terpenoids, flavonoids, proteins, sugars, and alkaloids, which act as reducing and capping agents [52]. Earlier research reported the green synthesis of TiO_2 nanoparticles using various plant extracts such as *Baccaurea racemosa* peel [53], *Butea monosperma* flower [54] *Citrus limon* leaf [55], *Myristica fragrans* seed [56].

The plant *Corchorus olitorius* (*C. olitorius*) Which is known colloquially as "molokhia", is one of the most common culinary and medicinal herbs widely used in several countries in the Middle East and North Africa [57]. The leaves of *C. olitorius* plant have been used for about 2,500 years by the ancient Egyptians and Indians as a nutritious vegetable, as well as to treat fever, sore throat, diarrhea and vomiting [58]. *C. olitorius* belongs to the Tiliaceae family, and its leaves are rich in antioxidants, such as vitamin C, vitamin E, beta-tocopherol, alpha-carotene, glutathione, and phenols. It also contains fatty acids, other vitamins, minerals, and mucopolysaccharides [59]. *Corchorus olitorius* has demonstrated a broad spectrum of biological activities, which are undoubtedly associated with its phytochemical constituents. Molokhia leaves are commonly utilized in traditional medicine due to the belief in their notable nutritional and therapeutic benefits for treating various diseases and disorders [60]. Recent research indicates that *Corchorus olitorius* possesses anti-inflammatory and anti-proliferative properties, as demonstrated in various in vitro and in vivo studies [61]. As well as ointments made from powder and aqueous extract of *C. olitorius* leaves also showed promise results in promoting wound healing [62]. The plant *C. olitorius* is widely used in the textile industry, where the distinctive green color of natural dyes extracted from its leaves is used to color textile materials such as cotton [63].

Based on the above facts, *C. olitorius* leaves extract is considered a better candidate for the green synthesis of nanoparticles. Many nanoparticles were successfully synthesized using *C. olitorus* leaves as a reducing, capping, and stabilizing agent such as gold nanoparticles, copper (II) oxide nanoparticles, and carbon dots [64-66]. However, there are no reports available on the fabrication of TiO_2 nanostructures using *C. olitorius* extract. In this work, *Corchorus olitorius* leaf extract were successfully used to synthesize titanium dioxide nanoparticles for the first time. The produced TiO_2 nanoparticles were identify and their properties were studied using various techniques. The prepared TiO_2 nanoparticles were used as photocatalyst and their photocatalytic activity was investigated for the degradation of methylene blue dye and Tetracycline in aqueous solution as a model pollutant under sunlight. For comparison, photocatalytic test was performed under ultraviolet light. The prepared pure

titanium dioxide nanoparticles demonstrated unprecedented decomposition efficiency towards methylene blue and tetracycline under natural sunlight.

2- Materials and methods

2.1. Materials

High purity Titanium tetraisopropoxide –TTIP ($C_{12}H_{28}O_5Ti$, 98%) was purchased from (MSB CHEMICAL LIMITED, India) as a titanium source. The dry leaves of molokhia were obtained from the Baghdad local market, Iraq. Methylene Blue dye ($C_{16}H_{18}ClN_3S$) was purchased from Sigma-Aldrich. Tetracycline antibiotic ($C_{22}H_{24}N_2O_8$) was purchased from a local pharmacy, Iraq. Ethanol (99% C_2H_5OH) from (MSB CHEMICAL LIMITED, India) Deionized water was used to prepare all solutions.

2-2 *Corchorus Olitorus* leaves extract preparation

Leaf extract can be obtained by various methods. Both cold and hot methods were combined to prepare the molokhia extract [67]. Thoroughly dried molokhia leaves were washed with deionized water three times to remove dust. Twenty grams of clean leaves were soaked in 400 ml of deionized water for 24 hours, then the mixture was heated to 75°C for three hours. The extract was then filtered in two stages: first through a sieve to remove large particles, and second through Whatman filter paper No. 1. The purified filtrate was stored in a refrigerator for later use in the synthesis of titanium dioxide nanoparticles.

2-3 Green synthesis of TiO_2 NPs

To produce titanium dioxide (TiO_2) nanoparticles, 20 mL of titanium tetraisopropoxide (TTIP) added drop-wise to 200 mL of molokhia extract while stirring continuously for 2 hours using a magnetic stirrer at room temperature. The resulting solution was then washed three times with deionized water and ethanol using a centrifuge at 4000 rpm for 15 minutes each time. The product was thoroughly dried on a hot plate at 100°C for 1 hour, forming a yellowish powder. The powder was then calcined at 450°C for 3 hours, resulting in a white powder after calcination.

2-4 Characterization

The structural characteristics of greenly synthesized TiO_2 NPs were analyzed using a powder X-ray diffractometer (SHIMADZU XRD-6000, Japan). Field emission scanning electron microscopy (TESCAN MIRA3, French) coupled with EDX was used to analyze the surface morphology and determine the elemental composition of TiO_2 nanoparticles. Fourier transform infrared (FTIR) spectroscopy (Bruker, Germany) was performed to investigate the molecular vibration and functional groups of molokhia leaves and TiO_2 NPs. The room temperature PL spectrum of TiO_2 NPs was recorded using a spectrofluorophotometer (RF-5301PC, Shimadzu) with an excitation wavelength of 325 nm. Zeta potential measurements was preformed using Zetasizer Nano (ZS, Malvern Panalytical, UK). A UV–Vis spectrophotometer (Lasany Double Beam LI-2800, India) was used to study the optical properties of the synthesized TiO_2 NPs and monitor the degradation of MB dye and TC antibiotic.

2-5 Photocatalytic activity of TiO_2 NPs for MB dye and TC antibiotic degradation

To study the photocatalytic activity of titanium dioxide nanoparticles, methylene blue dye and the antibiotic tetracycline were used as model pollutants under both UV and sunlight. Ten milligrams of TiO_2 nanoparticles were added to 50 mL of an aqueous solution containing methylene blue (MB) dye at a concentration of 10 mg/L. The reaction mixture was kept in the dark with continuous stirring for 60 min until adsorption-desorption reached equilibrium. The reaction mixture was exposed to natural

sunlight from 11:30 am to 12:30 pm Baghdad time in August 2025. To reduce the effect of ambient temperature, which was about 47°C ± 2, the mixture was cooled down using a water bath to maintain a constant temperature of approximately 30°C ± 2. To monitor the kinetics of methylene blue (MB) degradation, 3 mL of the reaction mixture were withdrawn every 10 minutes. Each sample was then centrifuged for 10 minutes at 4,000 rpm. The absorbance spectra for the reaction mixture were recorded. The previous steps were repeated under UV light using a CAMAG UV lamp with a wavelength of 366 nm. For the TC decomposition reaction, 10 mg of titanium dioxide nanoparticles were added to 100 mL of aqueous TC solution (50 mg/L). The mixture was kept in the dark for 30 minutes and then exposed to natural sunlight and UV light (366 nm). After a specified time of 20 minutes, the test sample was withdrawn and filtered through a 0.22 μm disposable syringe filter. The filtered sample was then analyzed using UV-Vis spectroscopy to determine The degradation of TC antibiotic.

The degradation percentage of both pollutants and first-order rate constant (k) were calculated by the following equations:

$$Percentage\ degradation\ (\%) = \frac{Co - C}{Co}\ x\ 100\% \qquad (1)$$

$$ln\ \frac{Co}{C} = kt \qquad (2)$$

where C_0 and C represent the initial and time-dependent pollutant concentrations.

3- Results and discussion

3-1 X-ray diffraction analysis (XRD) of TiO_2 NPs

The structural properties of green synthesized titanium dioxide nanoparticles using Molokhia leaf extract were studied using X-ray diffraction patterns, shown in Figure 1. The characteristic diffraction peaks observed at 2θ values of 25.58°, 38.28°, 48.18°, 54.81°, 63.06°, 69.70°, and 75.57° correspond to crystallographic planes (101), (112), (200), (105), (204), (220), and (215), respectively, confirming the anatase phase of TiO_2 nanoparticles with tetragonal structure, as indicated by JCPDS reference No. 00-002-0406, with lattice parameter a = b = 3.73Å, c = 9.36Å, and cell volume v = 130.22 $Å^3$. The slight difference between the standard (a = b = 3.77 Å, c = 9.48 Å, and v = 135.25 $Å^3$) and calculated values of the lattice parameters indicates the presence of some strain in the lattice that can be attributed to the preparation method and nanocrystallites formation [68]. No peak of rutile or brookite phase was observed. Here lies the importance of green synthesis methods that utilize the functional groups present in the molokhia extract to obtain the most photoactive phase of titanium dioxide. The absence of diffraction peaks due to impurities is evidence of the high purity of the prepared nanoparticles. The crystallite size of TiO_2 NPs was calculated for a dominant peak at a 2θ value of 25.58° for the (101) crystal plane using the Scherer equation (Eq. 3) and was found to be 7.48 nm. The small crystal size value indicates the superiority of molokhia leaf extract in the synthesis of small nanocrystals compared to other plant extracts, as reported in previous literature [37,39]. The XRD pattern exhibits relatively sharp dominant diffraction peak despite the small crystallite size estimated from peak broadening, indicating the presence of extended coherent scattering domains rather than isolated, randomly oriented nanoparticles. Other crystallographic parameters including microstrain and dislocation density, were calculated for the (101) crystal plane using equations (4) and (5), respectively. Both the calculated strain value which is 20.8×10^{-3}, and the dislocation density which is 1.78×10^{16} $lines.cm^{-2}$ indicate the presence of slight deformations that can be attributed to the nanocrystals. These results confirm the good crystallinity of the green synthesized TiO_2 NPs.

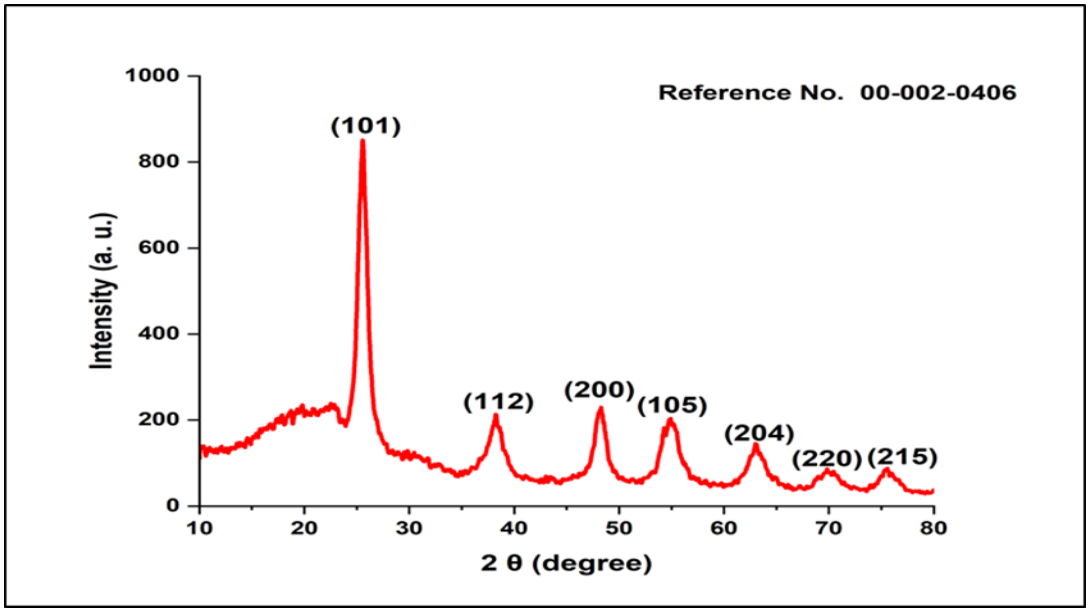

Fig (1): X-ray diffraction pattern of TiO_2 NPs

$$D = \frac{k\lambda}{\beta cos\theta} \quad (3)$$

$$\varepsilon = \frac{\beta}{4tan\theta} \quad (4)$$

$$\delta = \frac{1}{D^2} \quad (5)$$

Where D: crystallite size is k: shape factor = 0.9, λ: x-ray wavelength = 1.5406Å, β: full width at half maximum (FWHM), θ: diffraction angle, ε: strain, and δ: dislocation density.

Williamson-Hall (W-H) analysis was also utilized to calculate crystallite sizes and lattice strain using equation 6. Figure 2 shows the W-H plot, indicating that the calculated crystallite size value is 9.03 nm, which is slightly larger than the value calculated from Scherrer equation, where the inclusion of the lattice strain increases the crystallite size value. The calculated lattice strain was 0.00548 × 10^{-4}.

$$\beta\ cos\theta = \frac{k\lambda}{D} + 4\varepsilon\ sin\theta \quad (6)$$

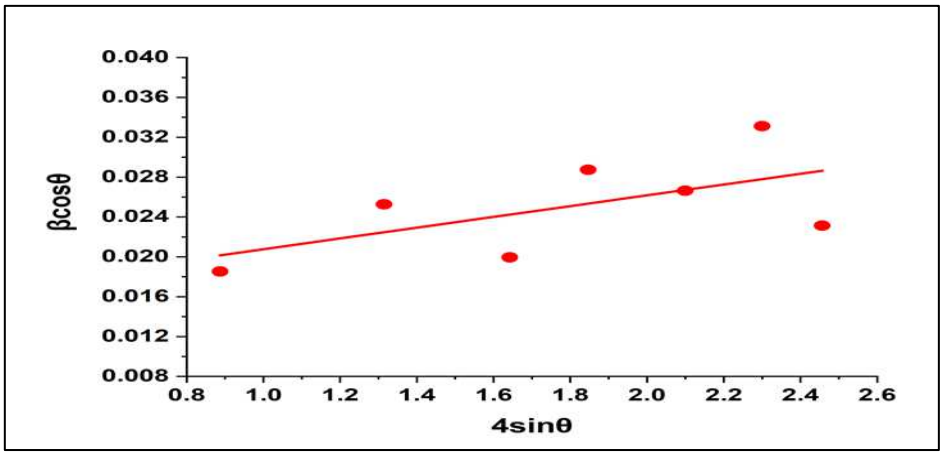

Fig (2): Williamson-Hall plot of TiO_2 NPs

3-2 FTIR analysis of TiO_2 NPs

The presence of functional groups and chemical bonds in the green synthesized TiO_2NPs and Molokhia leaves extract was investigated using FTIR analysis, as shown in Figure (3). The FTIR spectrum of molokhia extract confirms the presence of a range of chemical bonds and active groups. A broad band centered at 3272 cm^{-1} is attributed to stretching vibrations of the hydroxyl group (OH), possibly from the phenolic components. Stretching vibrational bonds (C-H) belonging to the aliphatic groups CH_2 and CH_3 were also observed at 2917 cm^{-1} and 2849 cm^{-1}, respectively. C-O stretching vibration (amide) and C-C stretching from phenyl groups and COO symmetric stretching were located at 1603 cm^{-1}. A peak at 1239 cm^{-1} corresponding to ester sulfate groups (S=O). C-O stretching was noticed at 1022 cm^{-1}. At least the peak at 530 cm^{-1} corresponds to C-O-C and C-C vibrations of polysaccharide in cellulose, hemicellulose, and mucilage. These results are consistent with the findings of previous studies [69,70]. The presence of many phytochemical compounds in molokhia extract proves its potential use as a reducing and capping agents for the production of small-sized TiO_2NPs. The FTIR spectrum of TiO_2NPs shows the presence of a weak broad peak at 3344 cm^{-1} that corresponds to hydroxyl group (OH) stretching vibrations. This is attributed to water absorbed on the surface. A band at 1586 cm^{-1} corresponding to the bending vibration of the Ti–OH group was also confirmed. The broad peak observed at 430 cm^{-1} represents stretching vibrations of Ti–O and Ti–O–Ti bonds and confirms the formation of TiO_2 nanoparticles. The absence of any peaks corresponding to the organic group confirms the high purity of the sample, as the lack of any organic species indicates that it was completely combusted during the calcination process[71].

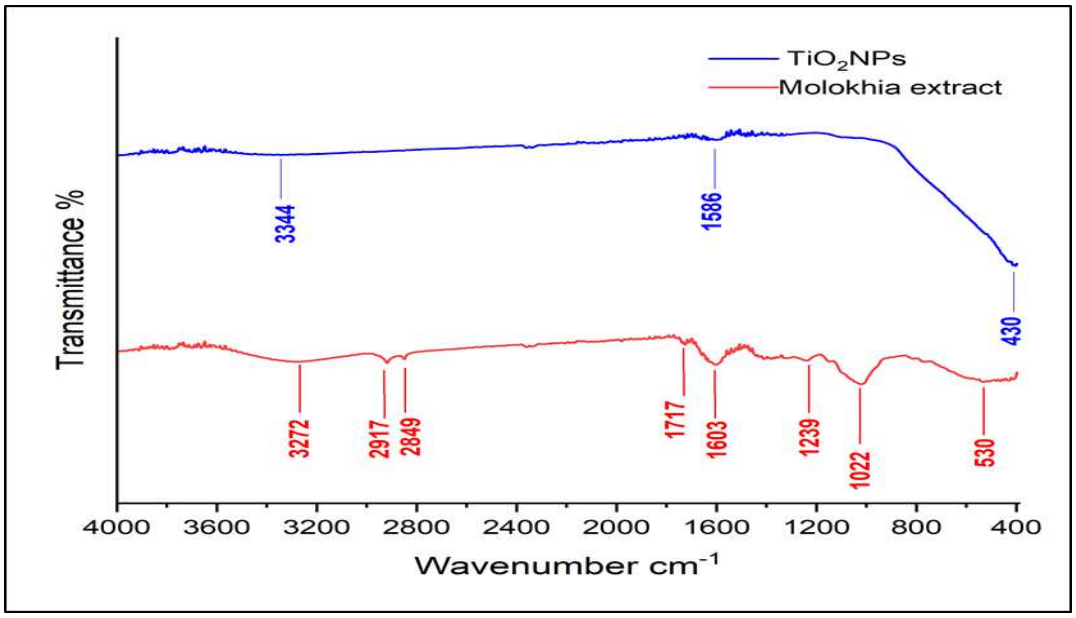

Fig (3): FTIR spectra of TiO_2 NPs and molokhia extract

3-3 FESM analysis of TiO_2 NPs

The field-emission scanning electron microscopy images of TiO_2 NPs with different magnifications are shown in Figure (4). According to low-magnification FESEM images (Figure 4-a, -b, -c), titanium oxide clearly exhibits a porous structure with open-ended tubular channels of about 1.94 µm in diamete, while high-magnification images (Fig.4-d) reveal that the structure consists of uniformly distributed, spherical nanoparticles with average particle size of about 20 nm (The dimensions were calculated using ImageJ software). FESEM observations reveal well-defined micro/submicroscale architectures composed of nanoscale surface features, suggesting an assembly of nanosized building blocks rather than dense bulk crystals. The formation of the microporous / mesocrystal like structure can be attributed to the presence of mucopolysaccharides in the molokia extract, which act as a natural bio template during the preparation

process[72].After calcination at 450 ºC for three hours, the bio-template was removed leaving porous structures around the TiO_2 NPs [73]. The presence of small nanoparticles is an indication of the success of the phytochemicals found in the extract of molokia leaves as a caping agent that maintains a small size and prevents the formation of nanoparticle aggregation .The porous structures exhibit ideal transport pathways for introducing the liquid phase of pollutants into the titanium dioxide catalyst, while nanosized particles provide a large surface area which increases the number of active sites. The synergistic role of this microporous / mesocrystal like structure enhances photocatalytic efficiency of TiO_2 NPs.

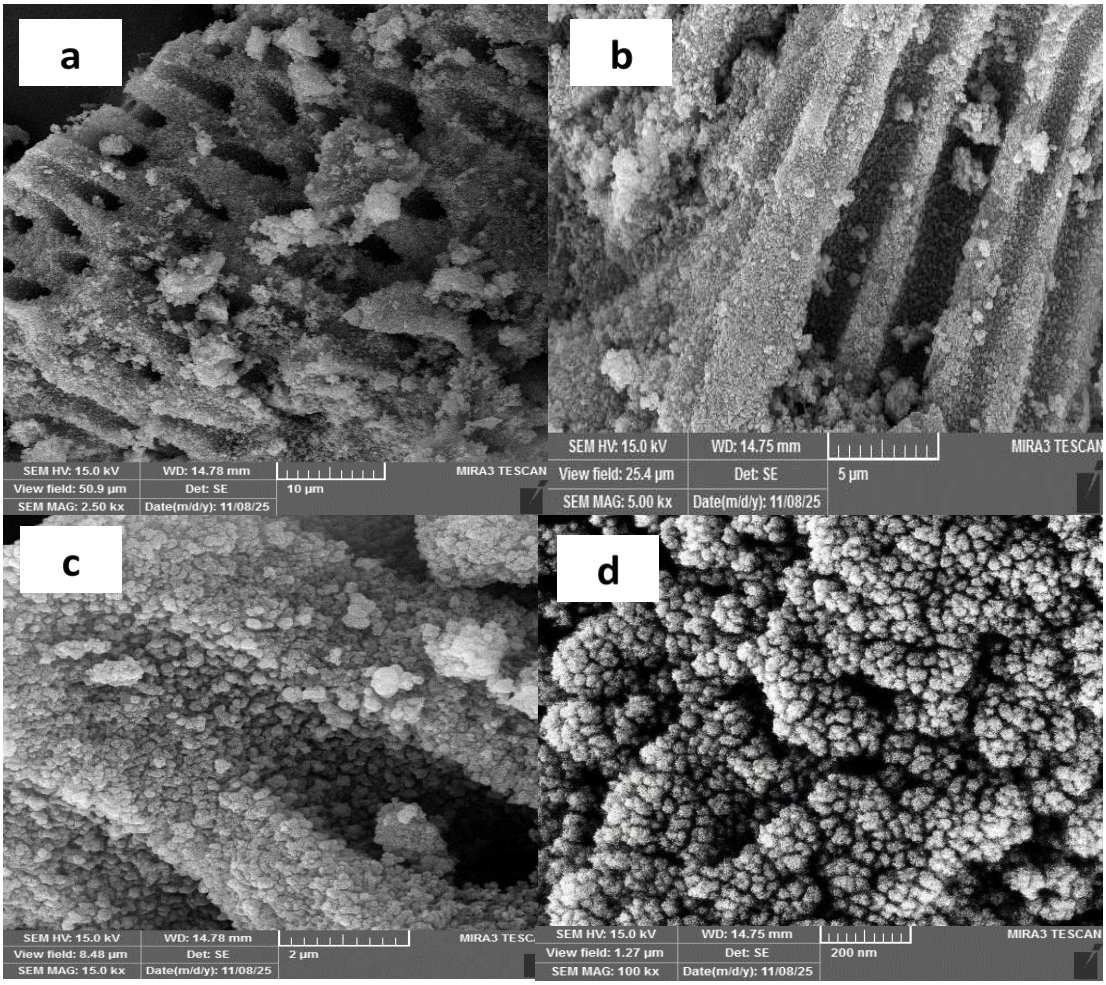

Fig (4):FESEM images of TiO_2 NPs with different magnification

3-4 EDX analysis of TiO_2 NPs

The percentage of elements present in the prepared TiO_2 NPs was evaluated using energy dispersion spectroscopy (EDX). Fig. (5-a) shows the EDX spectrum of TiO_2 NPs, which confirmed the existence of titanium and oxygen peaks. The table inset of fig. (5-a) listed the atomic and weight percentage of each element. There are no additional peaks in the EDX spectrum, which confirms the absence of impurities in the green synthesized nanoparticles. Figure (5-b, -c, -d) shows a mapping distribution of elements in the selected area of the sample, where a homogeneous distribution of elements is observed, in accordance with the atomic and weight percentage of each element as specified in the table.

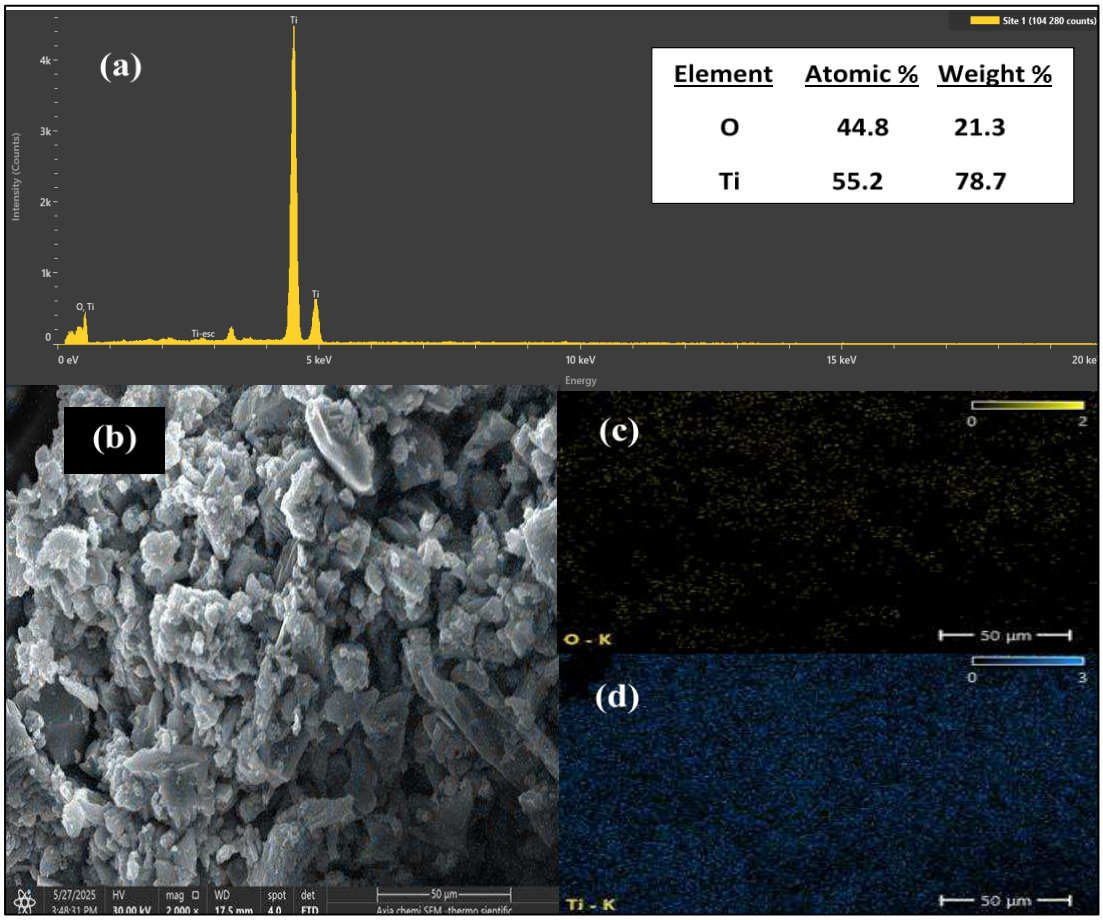

Fig (5): EDX spuctrum of TiO_2 NPs (a),mapping elements (b-d)

3-5 Photoluminescence (PL) nalysis of TiO_2 NPs

Photoluminescence (PL) spectrum provide us with a way to understand the electronic structure of semiconductors, determine the energy gap, and assess the presence of defects. The PL spectrum of TiO_2 NPs is shown in Figure (6). Photoluminescence spectrum exhibit reduced emission intensity and peak narrowing, implying suppressed nonradiative recombination associated with excessive grain boundaries.A strong emission peak was observed in the ultraviolet region centered at 378 nm, belong to the near-band egde emission (NBE), while two weak peaks were also present in the visible region. A narrow blue emission peak positioned at 471 nm ,which is originated from defect related states like oxygen vacancies .The broad near infrared emission peak centered at 746 nm is attributed to deep –level defect states mainly oxygen vacancies and Ti^{3+} present within the bandgap of TiO_2 NPs. These results are consistent with what has been published in the literature [74]. These defects play a crucial role by capturing photogenerated electron-hole pairs and preventing their recombination, thus enhancing the efficiency of photocatalsis.

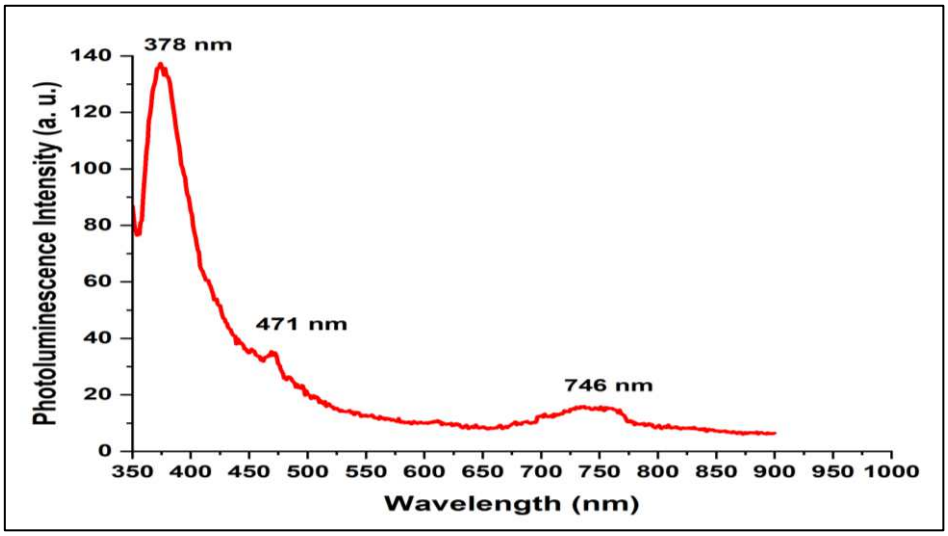

Fig. (6) Photoluminescence spectrum of TiO_2 NPs

3-6 Zeta potential result of TiO_2 NPs

The surface charge (zeta potential ζ) is an important index which reflects the stability of nanoparticles dispersion. The surface charge of TiO_2 NPs was mesured to detrmined their stability in suspension and adsorption properties of their surfaces.Figure (7) shows the zeta potential distribution of green synthesized TiO_2 nanoparticles in aqueous suspensions, the mean value was found to be -31.8 mV. The negative value of zeta potential indicate that the nanoparticles surface has negative charge. The negative charge can be attributed to presence of negative functional groups on the surface like, – OH-, – O-, and – COO-, which is common in nanoparticles prepared using the green method or dissociation of surface hydroxyl groups Ti – O [75]. The high zeta potential value (|ζ|> 30 mV) the high stability suspensions and low agglomeration nanoparticles due to highly electrostatic repulsion[76]. In addition, the negatively charged surface attracts positive ions and enhances their absorption on the catalyst surface, which promotes the photocatalysis process.

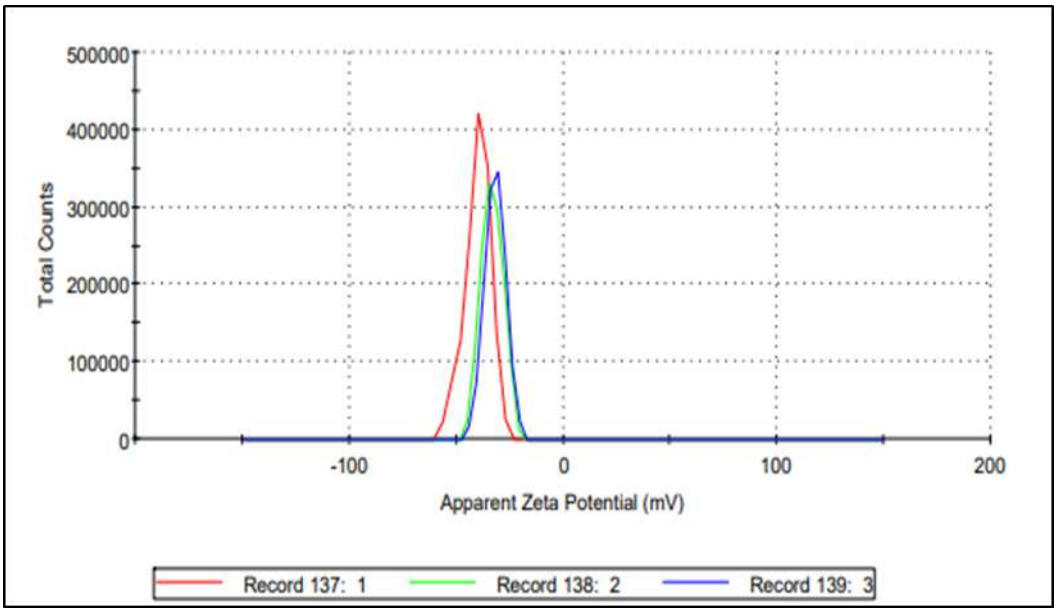

Fig. (7) Zeta potential distribution of TiO_2 NPs

3-7 Optical properties of TiO_2 NPs

The optical properties of TiO_2 NPs were characterized using UV-Vis spectroscopy, with the results presented in Figure (8). Figure (8-a) shows the absorption spectrum of TiO_2 NPs where a well-defined absorption edge was observed, associated with broad and strong absorption in the ultraviolet region and a limited-band tail. The band gap energy was estimated by extrapolation from the Tauc plot (Figure 8-b) described by the equation (7).

$$(\alpha h\nu)^n = A(h\nu - Eg) \qquad (7)$$

where α is the absorption coefficient, h is the Planck's constant, ν is the photon frequency, A is a proportionality constant, Eg is the band gap, and n is equal to 2 or 1/2 for allowed direct and indirect transitions, respectively. As is known from previous literature, titanium oxide is a semiconductor material with an indirect energy gap [77]. The calculated indirect energy gap for titanium dioxide nanoparticles was found to be 3.26 eV. The obtained band gap agrees well with that of the anatase phase reported in previous literature[78].

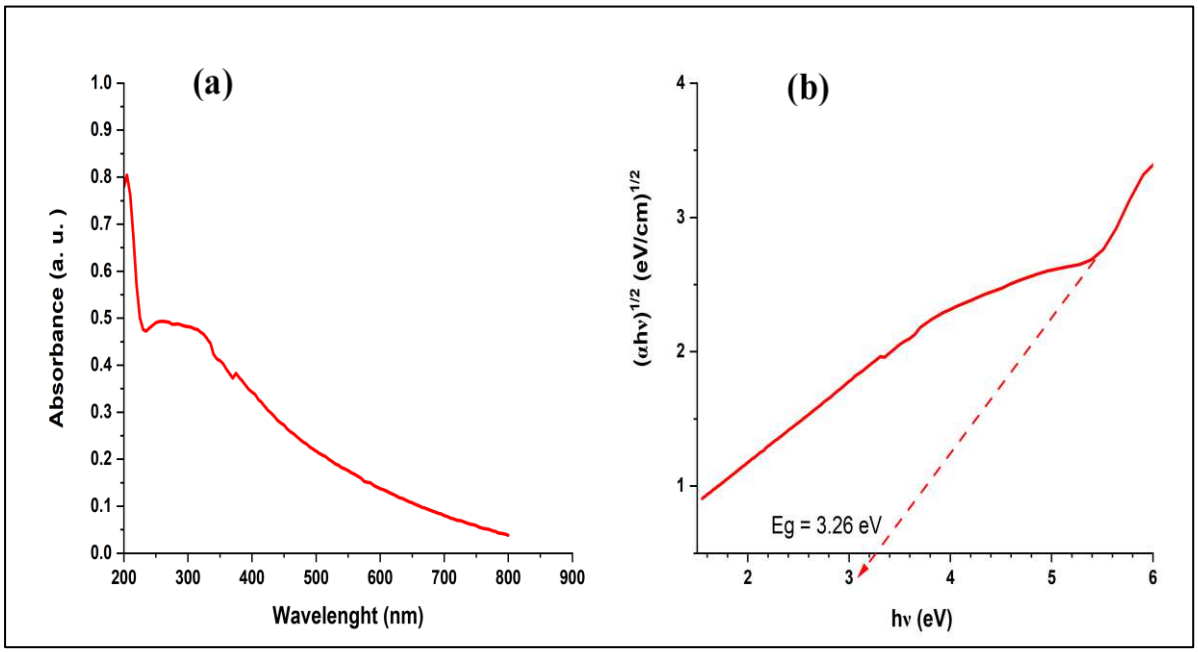

Fig.(8): absorption spectrum of TiO_2 NPs (a), Tauc plot(b)

3-8. Photocatalytic Activity of TiO_2 NPs

The photocatalytic performance of the synthesized TiO_2 NPs was evaluated against both MB dye and TC antibiotic under exposure to UV and sunlight irradiation. The degradation of MB was evaluated by monitoring the change in the maximum absorption peak at 664 nm. The gradually decreased of maximum absorption peak of the MB dye after continuous exposure to ultraviolet radiation and sunlight was observed, as shown in Figure (9-a, -b) respectively. The decrease in absorbance value can be attributed to a decrease in dye concentration, which is consistent with Lambert-Beer's law, indicating the decomposition of methylene blue molecules. The color change of methylene blue dye with increasing exposure time to light has been shown in images inset Figure (9-a, -b). This is a rapid and visible indicator of the dye's photodegradation, as a gradual color shift was observed from dark blue to light blue, culminating in the complete disappearance of the blue color when exposed to sunlight compared to ultraviolet radiation. The disappearance of the blue dye color is resulting from destroyed the chromophoric structure of dye [79]. The degradation percentage increase with increasing the exposure time (fig. 9–c) and reaches 77.8% after 80 min of exposure to UV light, which is slightly greater than

that reported value of pure TiO_2 [32,33,80]. The decomposition efficiency witnessed a remarkable increased under natural sunlight, where the dye decomposition percentage reached 97.5% after 80 min. (fig 9–c). This high efficiency of pure titanium dioxide nanoparticles towards methylene blue decomposition under sunlight has not yet been reported. The first-order rate constant k (fig. 9-d) and regression R^2 were found to be 0.02 min^{-1} and 0.97 in the case of ultraviolet radiation exposure, while there were 0.05 min^{-1} and 0.98 for solar light. The rate constant for degradation under sunlight was found to be ~1.5 times faster than that under UV light.

The degradation reaction of TC was studied via exposure to UV and sunlight by monitoring the change in absorbance at the maximum wavelength of tetracycline (λ_{max} = 355 nm); results were displayed in Figure10. A decrease in absorbance value was observed with increasing exposure time to light, which is an indicator of the breakdown of antibiotic molecules (fig. 10-a, -b). A degradation percentage of 24% was obtained after 120 min of UV light exposure, while a 56% degradation percentage was obtained after 120 min of sunlight (fig. 10-c). These results are superior compared to other researches [34,35]. The first-order rate constant k (fig. 10-d) and regression R^2 were found to be 0.0014 min^{-1} and 0.81 under ultraviolet radiation exposure, while there were 0.006 min^{-1} (3.2 time faster than that under UV light) and 0.98 under solar light.

Table 1 shows a comparison between the photocatalytic activity of TiO_2 NPs towards methylene blue and tetracycline under natural sunlight obtained in our study and previous literature. Small doses of TiO_2 nanoparticles have yielded superior results compared to previous research over shorter time periods.

Table 1: Comparative performance of present work TiO_2 NPs with previous literature

Synthesis method	**Light source**	**TiO_2 dose (mg/L)**	**Pollutant**	**Pollutant concentration (mg/L)**	**Degradation efficiency (%)**	**Time (min)**	**Reference**
Sol-Gel	sunlight	400	MB	5	97	90	36
Microwave assisted –green synthesis	sunlight	-	MB	-	97	90	37
green synthesis	sunlight	-	MB	-	91.41	195	40
Acid Catalyzed Hydrolysis	simulated sunlight	500	TC	10	0.00	60	35
green synthesis	sunlight	200	MB	10	97.5	80	**Present work**
		100	TC	50	56	120	

The superior efficacy of green synthesized TiO_2 nanoparticles in degrading methylene blue dye and tetracycline antibiotic under natural sunlight, as opposed to ultraviolet radiation from a UV lamp, can be ascribed to the broad UV spectrum of sunlight. This broad spectrum corresponds to the absorption of TiO_2 nanoparticles. Furthermore, all the improvement in photocatalytic activity can be attributed to : i) the successful production of the most active phase "anatase " using Molokhia extract, ii) increases in the number of reaction sites due to the large surface area of greenly synthesized TiO_2 NPs, resulting from their small size, iii) increasing the surface defects represented by oxygen vacancies which confirm by PL results, which play an effective role in preventing recombination of photogenrated electron-hole pairs, iv) highly negative zeta potential, meaning that the suspension of TiO_2 NPs is stable and no agglomerating occurs during the photocatalytic process, overcoming the main obstacle to using titanium dioxide as a photocatalyst [81]. Finally, the high efficiency of methylene blue decomposition can be attributed to its increased adsorption onto the catalyst surface, as it possesses positively charged ions in aqueous solutions and is therefore attracted to the negatively charged surface of titanium oxide nanoparticles [5]. While the charge of tetracycline depends on the pH of the aqueous solution, being neutral at pH values greater than 3 and less than 7, and since the pH of the TC aqueous solution was approximately 6, its adsorption process was not affected by the negative surface charge due to the lack

of attraction between it and the surface of the nanoparticles [82]. Therefore, its decomposition efficiency was lower compared to methylene blue.

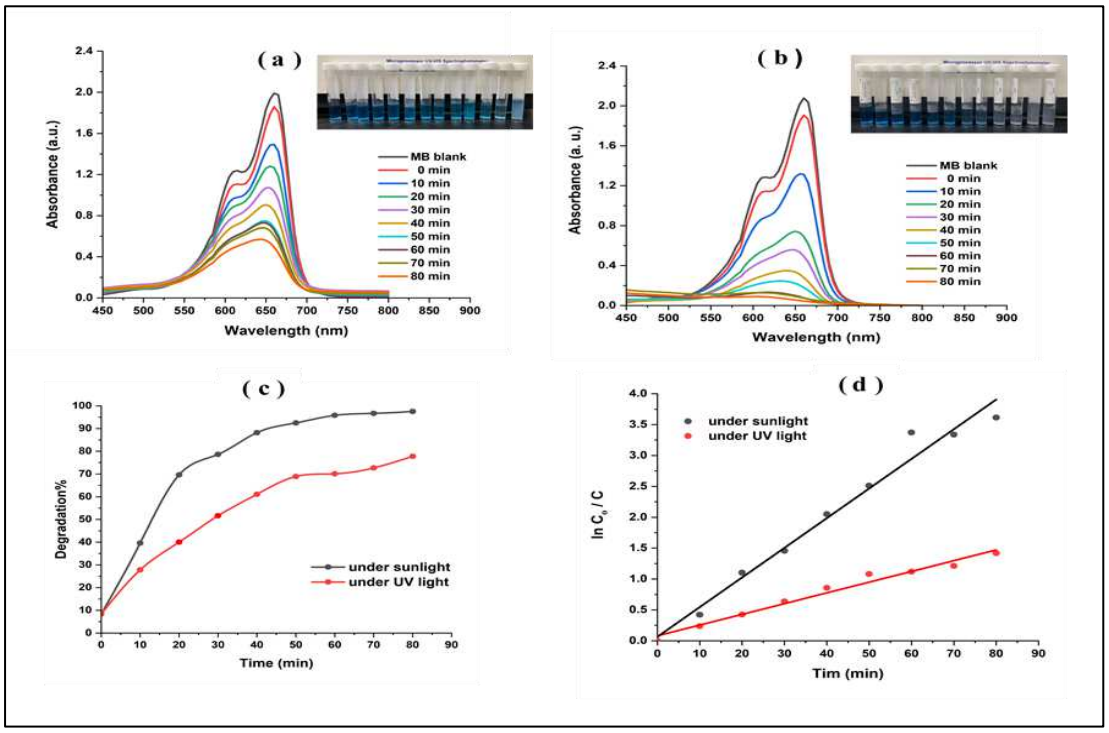

Fig. (9): Absorption spectra of MB dye under UV light (a), sun light (b), MB degradation % (c), ln C_o/C with time (d)

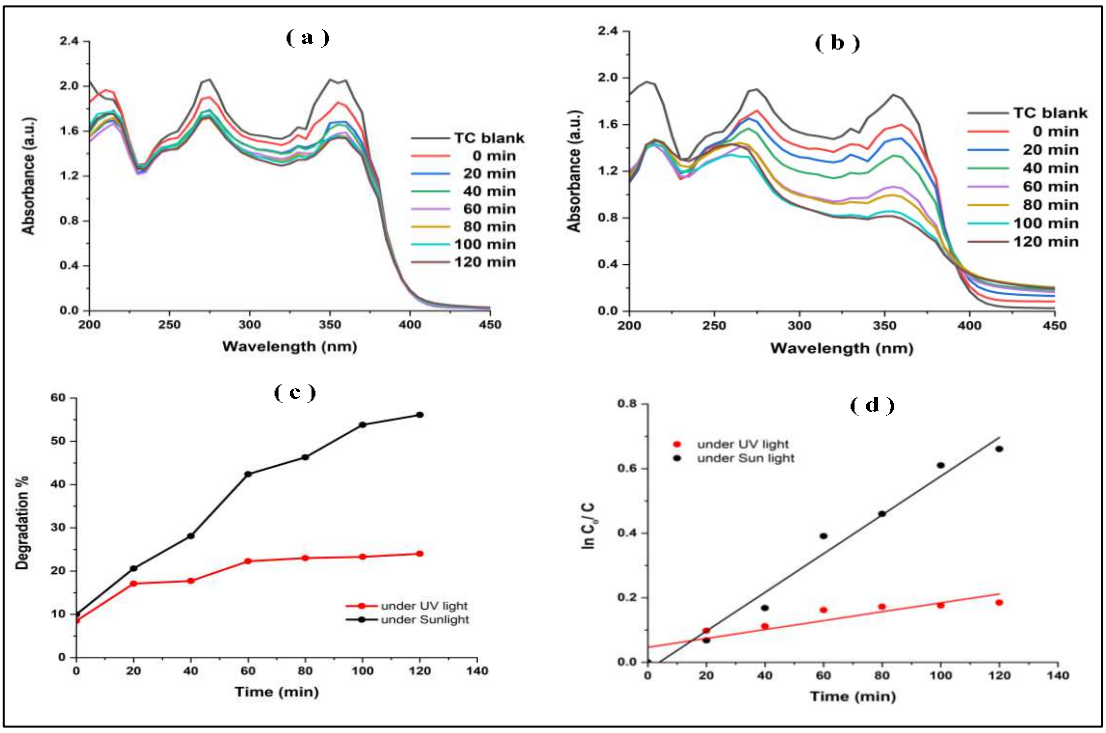

Fig (10): Absorption spectra of TC dye under UV light (a), sun light (b), TC degradation % (c), ln C_o/C with time (d)

3.9 Photodegradation mechanism of MB and TC using TiO_2 NPs

A potential process for the photodegradation of MB dye and TC antibiotic over produced nanoparticles exposed to both UV and sunlight was predicted following the reaction steps explained below. When light radiation with energy equal to or greater than the energy gap of TiO_2 NPs strikes their surface, electrons move from the valence band to the conduction band leaving a holes in the valence band. Photogenerated electron -hole pairs facilitate redox reactions at the catalyst surface, resulting in the formation of superoxide ions and hydroxyl free radicals. Photogenreted holes oxide the surface-adsorbed water molecules or hydroxide ions into hydroxyl radicals (•OH) while superoxide radicals ($\bullet O_2^-$) are produces by photogenreted electrons redaction of dissolved oxygen molecules. The penetration of these two active species into the functional groups of hazardous pollutants leads to the initiation of a series of reactions that result in the breakdown of harmful pollutants and their conversion into harmless substance such CO_2 and H_2O.

In addition to the mechanism mentioned above, there is another mechanism that can contribute to the breakdown of organic dyes and antibiotics under natural sunlight (~ 45% visible light content). The adsorbed MB dye and TC molecules on TiO_2 NPs surface absorbed a visible light undergoing electronic excitation under sun light [83,45]. Excited pollutant molecules inject electrons from the LUMO into the conduction band of TiO_2 nanoparticles, thereby enhancing charge carrier separation and increasing the formation of reactive oxygen species. These pollutants play as self-sensitizer enhancing the photocatalytic activity of TiO_2 NPs.

The reactions of the photodegradation mechanism can be summarized by the following equations and represented by the diagram in Figure 11.

$$TiO_2 + h\upsilon \rightarrow e_{CB}^- + h_{VB}^+ \quad (8)$$

$$h_{VB}^+ + H_2O \rightarrow \bullet OH + H^+ \quad (9)$$

$$h_{VB}^+ + OH^- \rightarrow \bullet OH \quad (10)$$

$$e_{CB}^- + O_2 \rightarrow \bullet O_2^- \quad (11)$$

$$\bullet O_2^- + H^+ \rightarrow HO_2^\bullet \quad (12)$$

$$2HO_2^\bullet \rightarrow H_2O_2 + O_2 \quad (13)$$

$$H_2O_2 \rightarrow 2 \bullet OH \quad (14)$$

$$MB + \bullet OH \rightarrow CO_2 + H_2O \quad (15)$$

Under sunlight illumination, additional reaction take place contributed to degradation of MB molecules.

$$MB + h\nu_{vis} \rightarrow MB^* \quad (16)$$

$$MB^* \rightarrow MB^+ + e^- \quad (17)$$

$$e^- + TiO_2 \rightarrow TiO_2(e^-) \quad (18)$$

$$TiO_2(e^-) + O_2 \rightarrow \bullet O_2^- \quad (19)$$

The above reactions also occur in the case of tetracycline degradation. As well as the adsorbed TC interact with TiO_2 NPs forming TC-TiO_2 complex which found to be enhanced the ability of TiO_2 to absorbed in the visible region [84].

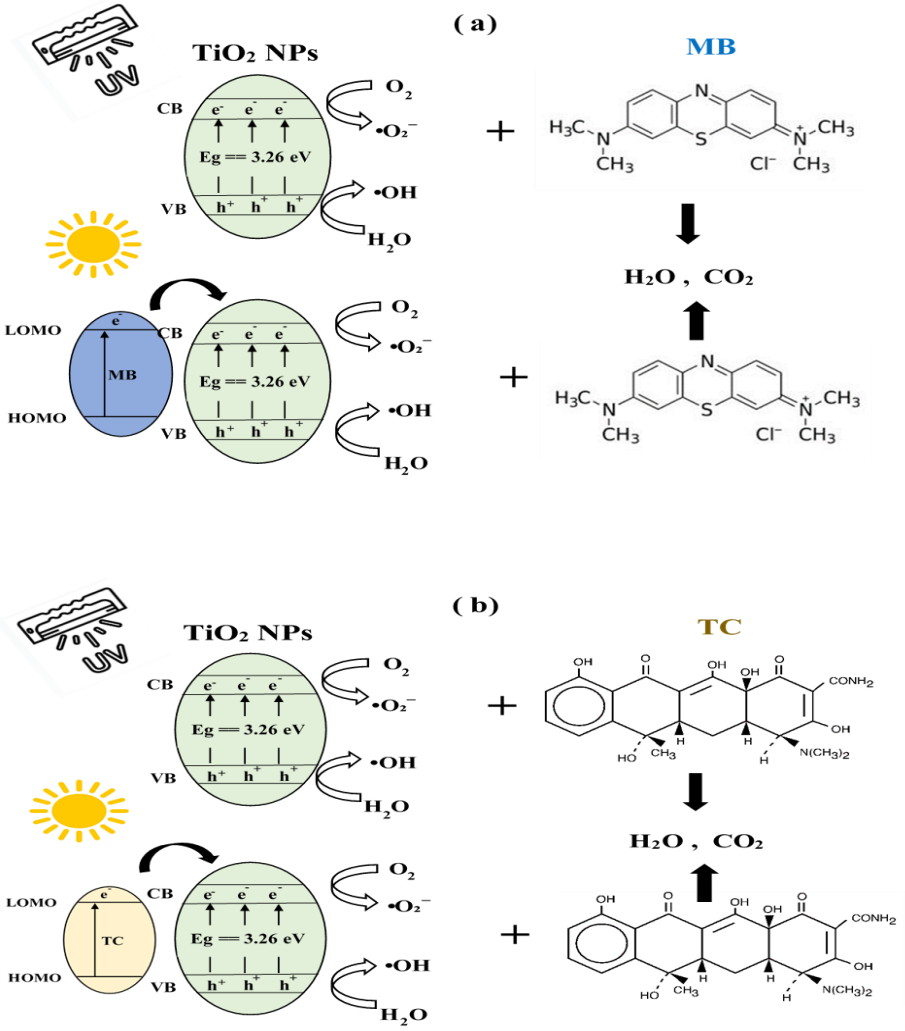

Fig (11): Schematic of photodegradation mechanism of MB (a) and TC (b)

Conclusion:

TiO_2 NPs were successfully synthesized via an innovative green method using an aqueous extract of molokia leaf. These NPs are created with distinctive characteristics by using the inherent phytochemical found in molokia. Anatase phase (the desired phase of TiO_2) was obtained with a particle size of less than 10 nanometers. These TiO_2 NPs show high absorbance in the UV region and presence of surface defect. High negative zeta potential value conforming their stability in colloidal solution. The plant compounds play an important role in determining the morphology of TiO_2 NPs, as the polysaccharides led to the formation of microporous structure. All these features led to improved photocatalytic efficacy of the prepared nanoparticles. They exhibited much higher efficiency for the photodegradation of MB and TC under sunlight than UV light, results not previously recorded with pure titanium dioxide.

Data availability statement: The manuscript has no associated data

Conflict of interest: The authors have no competing interests to declare that are relevant to the content of this article.

Funding: No funding was received to assist with the preparation of this manuscript.

References:

[1] P. O. Oladoye, T. O. Ajiboye, E. O. Omotola, O. Joel, Results Eng. 16 ,100678 (2022) https://doi.org/10.1016/j.rineng.2022.100678

[2] L. Zhang, J. Bai, K. Zhang, et al., J. Hazard. Mater. 457, 131751 (2023) https://doi.org/10.1016/j.jhazmat.2023.131751

[3] S. F. AbuQamar, M. T. El-Saadony, S. S. Alkafaas, et al, Mar. Pollut. Bull. 206, 116613 (2024) https://doi.org/10.1016/j.marpolbul.2024.116613

[4] A. Sahu, J. C. Poler, J. Environ. Chem. Eng. 12, 113754 (2024) https://doi.org/10.1016/j.jece.2024.113754

[5] B. Ahmadi, A. Fallah, R. Ghamarpoor, M. Jamshidi ,Results Chem. 18, 102910 (2025) https://doi.org/10.1016/j.rechem.2025.102910

[6] Y. Wang, Y. Wang, K. Zhao, et al., Environ. Pollut.382, 126739 (2025) https://doi.org/10.1016/j.envpol.2025.126739

[7] S. Wu, X. Li, Y. Tian, Y. Lin, Y. H. Hu, Chem. Eng. J. 406, 126747 (2021) https://doi.org/10.1016/j.cej.2020.126747

[8] X. Su, X. Zhang, L. Hu, et al., Sep. Purif. Technol. 353 Part C , 128614 (2025) https://doi.org/10.1016/j.seppur.2024.128614

[9] F. Ahmad, D. Zhu, J. Sun, Environ. Sci. Eur. 33, 64 (2021) https://doi.org/10.1186/s12302-021-00505-y

[10] J. Scaria, K.V. Anupama, P.V. Nidheesh, Sci.Total Environ. 771, 145291 (2021) https://doi.org/10.1016/j.scitotenv.2021.145291

[11] J.I. Mnyango, B. Yalala-Ndlovu, B. Nyoni, Next Mater.9, 100974 (2025) https://doi.org/10.1016/j.nxmate.2025.100974

[12] M. Minale, Z. Gu, A. Guadie, J. Environ. Manage. 276, 111310 (2020) https://doi.org/10.1016/j.jenvman.2020.111310

[13] Z. M. Hanafiah, W. H. M. W. Mohtar, R. Rohani, et al., J. Water Process Eng. 68, 106320 (2024) https://doi.org/10.1016/j.jwpe.2024.106320

[14] Y. Shi, Z. Yang, L. Xing, et al., World J. Microbiol. Biotechnol. 37, 137 (2021) https://doi.org/10.1007/s11274-021-03110-6

[15] Z. Kuspanov, B. Bakbolat, A. Baimenov, et al., Sci. Total Environ. 885, 163914 (2023) https://doi.org/10.1016/j.scitotenv.2023.163914

[16] M. A. Iqbal, S. Akram, S. khalid, et al., Environ. Res. 253, 118947 (2024) https://doi.org/10.1016/j.envres.2024.118947

[17] M. Muscetta, P. Ganguly, L. Clarizia, J. Enviro. Chem. Eng. 12 , 113073 (2024) https://doi.org/10.1016/j.jece.2024.113073

[18] F. Khodabandeloo, S. Shahsavarifar, B. Nayebi, et al., Inorg. Chem. Commun. 157, 111357 (2023) https://doi.org/10.1016/j.inoche.2023.111357

[19] A. K. Pandey, R. R. Kumar, B. Kalidasan, et al., J. Environ. Manage. 297, 113300 (2021) https://doi.org/10.1016/j.jenvman.2021.113300

[20] J. Salehzadeh, M. Nassiri, Z. Dehghani, S. Mohajeri, J. Indian Chem. Soc. 102, 102059 (2025) https://doi.org/10.1016/j.jics.2025.102059

[21] A. D. Nusseif, N. A. Hussain, R. S. Sabry , M. I. Rahmah, Next Nanotechnology 9 , 100396 (2026) https://doi.org/10.1016/j.nxnano.2026.100396

[22] C. Sun, J. Yang, M. Xu, et al., Chem. Eng. J. 427, 131564 (2022) https://doi.org/10.1016/j.cej.2021.131564

[23] Z. Li, J. Zhang, Y. Teng, et al., Inorg. Chem. Commun.155, 111060 (2023) https://doi.org/10.1016/j.inoche.2023.111060

[24] Y. Sari, P. L. Gareso, B. Armynah, D. Tahir, Int. J. Hydrogen Energy 55, 984-996 (2024) https://doi.org/10.1016/j.ijhydene.2023.11.126

[25] M. A. Kudhier, R. S. Sabry, Y. K. Al-Haidarie, Mater. Sci. Semicond. Process. 73, 35-41 (2018) https://doi.org/10.1016/j.mssp.2017.05.034

[26] J. Arun , S. Nachiappan, G. Rangarajan, et al., Environ. Chem. Lett. 21, 339-362 (2023) https://doi.org/10.1007/s10311-022-01503-z

[27] S. P. Sabino, E. B. Santos, B. I. M. Santos, M. Goncalves, Next Mater. 8 , 100856 (2025) https://doi.org/10.1016/j.nxmate.2025.100856

[28] N. S. N. Sa'ayaa, N. A. Halimb, H. A. Tajuddinc, et al., S. Afr. J. Chem. Eng. 53, 127–141 (2025) https://doi.org/10.1016/j.sajce.2025.04.014

[29] P. Kumari, S. Kumar, H. Kaur, et al., Interactions 245, 84 (2024) https://doi.org/10.1007/s10751-024-01918-w

[30] M. El Mchaouri, S. Mallah, D. Abouhajjoub, et al., Tetrahedron Green Chem 6, 100084 (2025) https://doi.org/10.1016/j.tgchem.2025.100084

[31] G. Nabi, Q. Ain, M. B. Tahir, et al., Int. J. Environ. Anal. Chem. 102, 434-442 (2022) https://doi.org/10.1080/03067319.2020.1722816

[32] F. Yang, C. Wang, L. Li, et al., Processes 13, 1192 (2025) https://doi.org/10.3390/pr13041192

[33] D. G. Mali, S. P. Patil, G. H. Sonawane, et al., Hybrid Advances 10, 100468 (2025) https://doi.org/10.1016/j.hybadv.2025.100468

[34] H. A. Ari, A. O. Aliyu, O. A. Alani, et al., Desalin. Water Treat. 320, 100819 (2024) https://doi.org/10.1016/j.dwt.2024.100819

[35] W. Cui, P. Wu, B. An, et al., Int. J. Biol. Macromol. 286, 138386 (2025) https://doi.org/10.1016/j.ijbiomac.2024.138386

[36] B. Bharatia, A. K. Sonkara, N. Singhb, et al., Mater. Res. Express 4, 085503 (2017) https://doi.org/10.1088/2053-1591/aa6a36

[37] A. Muthuvel, N. M. Said, M. Jothibas, et al., J. Mater. Sci: Mater. Electron. 32, 23522–23539 (2021) https://doi.org/10.1007/s10854-021-06840-3

[38] G. B. Yitagesu, D. T. Leku, G. A. Workneh, ACS Omega 8 , 43999–44012 (2023) https://doi.org/10.1021/acsomega.3c06142

[39] A. Singh, V. Goyal, J. Singh, M. Rawat, Curr. Res. Green Sustainable Chem. 3, 100033 (2020) https://doi.org/10.1016/j.crgsc.2020.100033

[40] A. M. Pillai, A. Harisankar, P. S. Salini, et al., Ionics 30, 4257–4270 (2024) https://doi.org/10.1007/s11581-024-05577-3

[41] S. Arunkumar, M. Alagiri, J. Clust. Sci. 28, 2635–2643 (2017) https://doi.org/10.1007/s10876-017-1245-6

[42] X. Zhang, H. Yu, Y. Song, et al., Appl. Surf. Sci. 640, 158403 (2023) https://doi.org/10.1016/j.apsusc.2023.158403

[43] Y. Li, W. Wang, F. Wang, et al., Nanomaterials 9, 720 (2019) https://doi.org/10.3390/nano9050720

[44] A. Khan, A. Tahira, K. P. Mahar, et al.,Results Chem.19, 102964 (2026) https://doi.org/10.1016/j.rechem.2025.102964

[45] Qi. Feng , S. Guo , Z. Bai ,et al., J. Ind. Eng. Chem. 145, 755–763 (2025) https://doi.org/10.1016/j.jiec.2024.10.072

[46] F. A. Sulaiman, A. I. Alwared, Desalin. Water Treat. 262, 312-322 (2022) https://doi.org/10.5004/dwt.2022.28504

[47] J. Roy, J. Ind. Eng. Chem. 106, 1-19 (2022) https://doi.org/10.1016/j.jiec.2021.10.024

[48] D. R. Eddy, D. Rahmawati, M. D. Permana, et al., Inorg. Chem. Commun. 165, 112531 (2024) https://doi.org/10.1016/j.inoche.2024.112531

[49] S. Q. Ali , W. J. Aziz , D. A. Kadhim , et al., Nano-Struct. Nano-Objects 39, 101257 (2024) https://doi.org/10.1016/j.nanoso.2024.101257

[50] C. Langa, N. C. Hintsho-Mbita, Chem. Phys. Impact 7, 100293 (2023) https://doi.org/10.1016/j.chphi.2023.100293

[51] H. Khan, S. Piccolella, S. Pacifico, Mater. Today Sustainability 31, 101195 (2025) https://doi.org/10.1016/j.mtsust.2025.101195

[52] A. Y. S. Zeebaree, S. Y. S. Zeebaree, R. F. Rashid, Curr. Res. Green Sustainable Chem. 5, 100312 (2022) https://doi.org/10.1016/j.crgsc.2022.100312

[53] Deliza, S. L. Rahayu, A. R. Liandi, R. A. Putri, S. Safni, Environ. Nanotechnol. Monit. Manage. 23, 101074 (2025) https://doi.org/10.1016/j.enmm.2025.101074

[54] S. D. Dhamale, A. R. Morey, P. V. Sawant, et al., Mater. Chem. Phys.: Sustainability and Energy 3, 100021 (2025) https://doi.org/10.1016/j.macse.2025.100021

[55] H. Kaur, S. Kumar, R. Saini, et al., Chemosphere 335, 139106 (2023) https://doi.org/10.1016/j.chemosphere.2023.139106

[56] S. Sagadevan, J. A. Lett, S. Vennila, et al., Chem. Phys. Lett. 771, 138527 (2021) https://doi.org/10.1016/j.cplett.2021.138527

[57] E. Bonnot, O. Claux, M. Boulkout, et al., LWT 232, 118393 (2025) https://doi.org/10.1016/j.lwt.2025.118393

[58] A. M. Metwaly, M. M. Ghoneim, I. H. Eissa, et al., Saudi J. Biol. Sci. 28, 5823-5832 (2021) https://doi.org/10.1016/j.sjbs.2021.06.044

[59] M. A. M. Abdel-Razek, M. F. Abdelwahab, U. R. Abdelmohsen, et al., RSC Adv. 12, 35103-35114 (2022) https://doi.org/10.1039/d2ra07406k

[60] H. Lee, M. Oh, M. H. Do, et al., J. Ethnopharmacol. 257, 112866, (2020) https://doi.org/10.1016/j.jep.2020.112866

[61] A. R. B. Yakoub, O. Abdehedi, M. Jridi, et al., Ind. Crops Prod. 118, 206-213 (2018) https://doi.org/10.1016/j.indcrop.2018.03.047

[62] K. Lee, J. H. Park, D. H. Lee, et al., Nat. Prod. Sci. 29, 291-296 (2023) https://doi.org/10.20307/nps.2023.29.4.291

[63] N. Bhouria, S. Ltaiefa, N. Bhouria, S. B. Abdessalema, J. Nat. Fibers 20, 2170946 (2023) https://doi.org/10.1080/15440478.2023.2170946

[64] E. H. Ismail, A. M. A. Saqer, E Assirey, et al., Int. J. Mol. Sci.19, 2612 (2018) https://doi.org/10.3390/ijms19092612

[65] R. O. Aljedaani, S. A. Kosa and M. Abdel Salam, Molecules 28, 16(2023) https://doi.org/10.3390/molecules28010016

[66] G. N. Kamel, R. A. Shabana, A. H. E. Hassan, R. El-Shaheny, Talanta 298, 128946 (2026) https://doi.org/10.1016/j.talanta.2025.128946

[67] J. Azmir, I. S. M. Zaidul, M.M. Rahman, et al., J. Food Eng. 117, 426-436 (2013) https://doi.org/10.1016/j.jfoodeng.2013.01.014

[68] I. Djerdj, A. M. Tonejc, J. Alloys Compd. 413, 159-174 (2006) https://doi.org/10.1016/j.jallcom.2005.02.105

[69] A. H. Abbas, G. Serikov, Y. Zhuniskenov, et al., ACS Omega 8, 29693−29703(2023) https://doi.org/10.1021/acsomega.3c03834

[70] M. Ghellam, B. Fatena, İ. Koca, Discov. Food 2, 14 (2022) https://doi.org/10.1007/s44187-022-00016-6

[71] P. S. Ramaripa , K.D. Modibane, W. M. Seleka, et al., Int. J. Electrochem. Sci. 19, 100444 (2024) https://doi.org/10.1016/j.ijoes.2023.100444

[72] N. Hammi, S. El Hankari, N. Katir, et al., Microporous and Mesoporous Mater. 306, 110429 (2020) https://doi.org/10.1016/j.micromeso.2020.110429

[73] S. S. Muniandy, N. H. M. Kaus, Z. Jiang, et al., RSC Adv. 7, 48083 (2017) https://doi.org/10.1039/C7RA08187A

[74] A. Sangeetha, A. Ambli, B.M. Nagabhushana, Nano-Struct. Nano-Objects 40, 101408 (2024) https://doi.org/10.1016/j.nanoso.2024.101408

[75] O. I. Salakoa, J. Jr. Gonzaleza, A. G. Cumminsa, et al., Surf. Interfaces 80 , 108180 (2026) https://doi.org/10.1016/j.surfin.2025.108180

[76] A. Rana, S. Parashar, D. Singh, et al., RSC Adv. 15, 9320-9334 (2025) https://doi.org/10.1039/D4RA08199D

[77] S. Landi Jr., I. R.Segundo, C. Afonso, et al., Physica B: Condensed Matter 639, 414008 (2022) https://doi.org/10.1016/j.physb.2022.414008

[78] K. M. Reddy, S. V. Manorama, A. R. Reddy, Mater. Chem. Phys.78, 239-245 (2003) https://doi.org/10.1016/S0254-0584(02)00343-7

[79] A. Saefumillah, D. O. B. Apriandanu, R. Ramadhan, et al., J. Mol. Struct. 1347, 143277 (2025) https://doi.org/10.1016/j.molstruc.2025.143277

[80] M. Mehenaoui, N. Chekir, D. Tassalit, et al., Eur. Phys. J. Plus 139, 1108 (2024) https://doi.org/10.1140/epjp/s13360-024-05849-x

[81] G. Li, L. Lv, H. Fan, et al., J. Colloid Interface Sci. 348, 342-347 (2010) https://doi.org/10.1016/j.jcis.2010.04.045

[82] Z. Li, L. Schulz, C. Ackley, N. Fenske, , J. Colloid Interface Sci. 351, 254-260 (2010) https://doi.org/10.1016/j.jcis.2010.07.034

[83] A.L.P.F. Caroni, C.R.M. de Lima, M.R. Pereira, J.L.C. Fonseca, Colloids Surf. B: Biointerfaces 100, 222-228 (2012) https://doi.org/10.1016/j.colsurfb.2012.05.024

[84] S. Wua, H. Hua, Y. Lina, et al., Chem. Eng. J. 382, 122842 (2020) https://doi.org/10.1016/j.cej.2019.122842